

Preparation of worm-like SiC nanofibers and their photoluminescence property

JIANYING HAO^{a,b}, YINGYONG WANG^b, XILI TONG^b, GUOQIANG JIN^b, XIANGYUN GUO^{b,*}

^aTaiyuan University of Science and Technology, Taiyuan, 030024, PR China

^bState Key Laboratory of Coal Conversion, Institute of Coal Chemistry, Chinese Academy of Sciences, Taiyuan 030001, PR China

The worm-like silicon carbide nanofibers were synthesized by simple carbothermal reduction technology. Low-cost water glass and phenolic resin were used as raw materials. The synthesized samples were characterized by XRD, FESEM, TEM, N₂ adsorption and fluorescence spectrophotometer. The results indicate that the products are worm-like β -SiC nanofibers with diameters of 20-110 nm. The maximum surface area of synthesized SiC is up to 51.6 m²/g. Strong photoluminescence peaks located around 450 nm and 468 nm are observed at room temperature, which can be ascribed to quantum size effects, microstructures and defects within the SiC materials.

(Received September 26, 2012; accepted June 12, 2013)

Keywords: Worm-like SiC, Carbothermal reduction, Nanofibers, Photoluminescence

1. Introduction

One-dimensional nanomaterials (e.g., nanowires, nanorods and nanotubes) have gained extensive attentions because of their unique properties and wide potential applications [1-3]. Among different nanomaterials, silicon carbide (SiC), as an important semiconductor and ceramic material, has been extensively studied due to its excellent physical, chemical, mechanical and electronic properties [4-6]. These properties make SiC attractive candidate materials for broad applications, such as reinforcement material, catalysis supports, electronic and optoelectronic nanodevices, field emission devices, nanosensors and photocatalysts [7-13], especially in harsh environments of high temperature, high power and high frequencies. It has been demonstrated that the size and morphology play a key role in determining the properties and applications of low-dimensional nanostructures [12]. Therefore, preparations of nanostructured SiC with a special morphology and structure become particularly important.

Currently, SiC nanomaterials with various morphologies such as nanowires, nanofibers, nanoparticles, nanobelts, nanorods, nanotubes, hollow sphere, etc [14-16] have been successfully synthesized using different preparation methods and raw materials. Zhang et al. [16] prepared SiC hollow spheres using sucrose and silicon powders as raw materials. Fu et al. [17] and Li et al. [18] synthesized SiC nanowires via chemical vapor depositions using CH₃SiCl₃, and Si, SiO₂, C₃H₆ as precursors, respectively. Sun et al. [19] prepared SiC nanotubes and nanowires via the disproportionation

reaction of SiO with carbon nanotubes. Seeger et al. [20] fabricated SiC whiskers by arc-discharge process of silicon and graphite powder. Eick [21] reported the synthesis of SiC nanofibers by pyrolysis of electrospun preceramic polymers. Xin et al. [22] prepared SiC nanomaterials with different morphologies (smooth nanowires, hierarchical nanodishes and short nanorods) by sol-gel carbothermal reduction method. Wang [23] synthesized SiC nanoparticles using foamed plastic wastes and tetraethoxysilane. Our group [7, 24-25] has successfully synthesized bamboo-like, chain-like and periodically twinned SiC nanowires by sol-gel and carbothermal reduction of a mixture of phenolic resin or biphenyl and tetraethoxysilane. In most cases, expensive raw materials, catalysts, and sophisticated techniques were used. These drawbacks may limit the massive fabrication and application of SiC nanomaterials. Consequently, the synthesis of nanostructured SiC by simple, efficient routes and economical raw materials is still a challenge. To our knowledge, the reports on using low-cost water glass as silica resource to synthesize SiC were few.

In this paper, we report a simple method for the large-scale preparation of worm-like β -SiC nanofibers. The synthesized SiC nanofibers have high BET surface area. This process has inherent advantages, including a simple preparation procedure, the low-cost raw materials, the lower synthesis temperature and the large-scale production. Moreover, the photoluminescence (PL) properties of the as-prepared SiC were studied, and strong violet-blue light emission was observed at room temperature.

2. Experimental

The synthesis process was briefly described as follows: 8 g of phenolic resin powders was mixed with water glass (containing 24.7wt% SiO₂, modulus = 3.33) under stirring according to different molar ratio of carbon to silicon. When molar ratio of carbon to silicon was 3/1, 3.5/1, 4/1, and 4.5/1, the as-prepared sample was in turn marked as C1, C2, C3, and C4, respectively. The mixture took a few minutes to turn into gel. The gel was dried at 80 °C for 12 h. The xerogel was heated in Ar flow (50 mL/min) to 1000 °C at a rate of 10 °C/min, then to 1300 °C at a rate of 2 °C/min and maintained at this temperature for 6 h in a horizontal tubular furnace. After the furnace was cooled down to room temperature, the obtained product was heated in air at 700 °C for 3 h to remove the residual carbon, and subsequently treated by the mixture of hydrochloric acid (HCl) and hydrofluoric acid (HF) for 48 h to eliminate the unreacted silica and other impurities. A light-green powder was obtained after washing with distilled water and drying.

The crystalline phases of the synthesized samples were characterized by X-Ray diffractometer (Philips X'Pert, XRD) using Cu K α radiation. The sample morphology was examined with S-4800 field emission scanning electron microscope (FESEM) and JEOL-1011 transmission electron microscope (TEM). The BET surface area was determined from nitrogen adsorption-desorption isotherms (at 77 K) using a Micromeritics ASAP-2000. The photoluminescence spectra were recorded with a Hitachi, F-7000 fluorescence spectrophotometer at room temperature, using a 370 nm Xe lamp excitation source and 430 nm cut filter.

3. Results and discussion

The formation of SiC precursor is substantially a dehydration reaction between water-soluble water glass and phenolic resin, which can transform the silica sol into the gel. Phenolic resin is acidic solid, while water glass is alkaline sol or viscous substance. For water glass, adjusting its PH value can make the gel formed. Therefore, we added acidic phenolic resin powders to adjust the PH value of water glass, and then the silica gel contained carbon was formed.

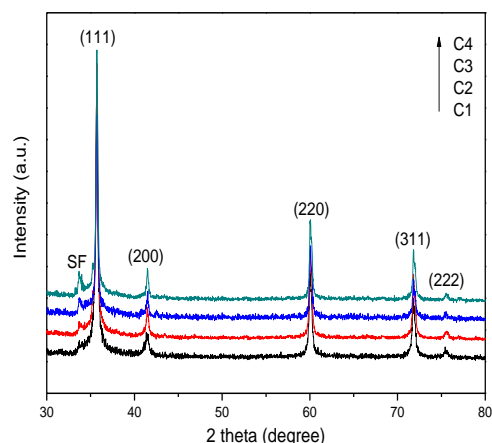


Fig. 1. XRD patterns of the SiC samples: C1-C4 represents the SiC samples with the molar ratio of carbon to silicon of 3/1, 3.5/1, 4/1 and 4.5/1, respectively.

The XRD patterns of different samples are shown in Fig. 1. As can be seen from the figure, all of the strong diffraction peaks can be indexed to cubic β -SiC and no other crystalline phases such as silica, carbon or other impurities are detected. The small peak marked with SF is attributed to stacking faults [26]. Strong and sharp diffraction peaks suggest that low-cost and facile water glass is an ideal silicon precursor to produce highly crystalline β -SiC. Although the XRD patterns of C1-C4 samples are similar, the diffraction peak intensity of stacking faults apparently strengthens with the increase of molar ratio of carbon to silicon, which is consistent with the analysis of the effect of carbon addition on stacking fault formation during carbothermal reduction [27]. It is well known that the particle size becomes smaller when there are more stacking faults in the materials. Hence, the synthesized products have smaller size with increasing molar ratio of carbon to silicon.

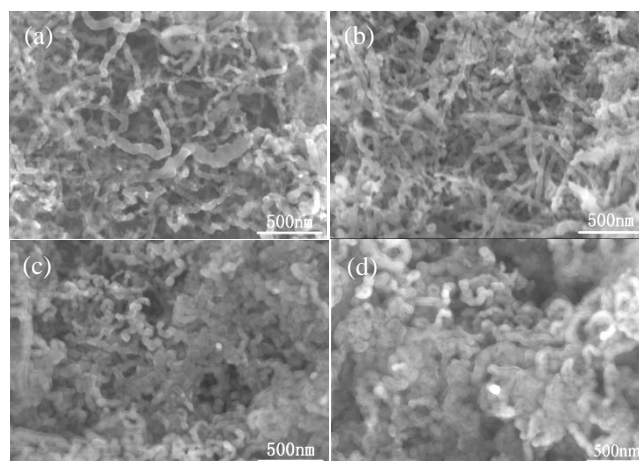


Fig. 2. SEM images of the SiC samples C1-C4 (a-d).

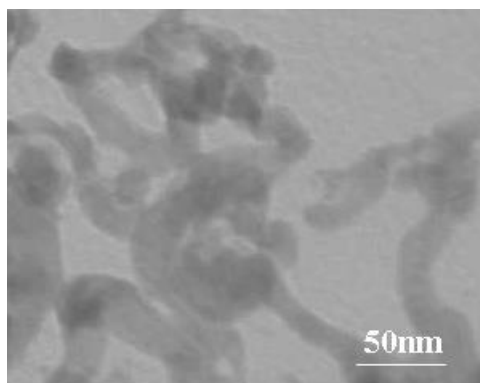


Fig. 3. TEM image of C3.

Typical SEM images of as-prepared SiC are displayed in Fig. 2a-d. It can be seen from Fig. 2a and 2b that the morphologies of C1 and C2 are similar, and both are vermiculate and crooked. Their surfaces are not smooth and have many knots. It can be calculated that most nanofibers of C1 sample have diameters in the range of 20-70 nm and lengths up to more than one micron, the diameters of few nanofibers are nearly 110 nm. While the diameters of C2 sample are lower than that of C1 sample, the biggest diameter of C2 sample is about 90 nm. The lengths of C2 sample are obviously shorter than that of C1 sample. SiC with these morphologies have great potential applications in composites, because these knots can greatly improve the strength of composites through strong interfacial adhesion with matrix. When the molar ratio of carbon to silicon reaches 4 and 4.5 (as shown in Fig. 2c and 2d), the surfaces of synthesized SiC gradually become smooth and the diameters become uniform, but the morphologies are still crooked and worm-like.

In order to further confirm the uniform vermiculate morphologies, the typical TEM image of C3 is displayed in Fig. 3. The diameters of these smooth nanofibers are about 20-60 nm, lower than that of C1 and C2, and the lengths are less than one micron.

The above results illustrate that with the increase of the molar ratio of carbon to silicon, the morphology of prepared SiC becomes smooth, which can be attributed to carbon addition and impurities content of industrial water glass. The contact areas between carbon and silica increase with the increase of the molar ratio of carbon to silicon, the carbothermal reduction reactions become complete. Moreover, taking into account the composition of water glass, according to the phase diagram of $\text{Na}_2\text{O}-\text{SiO}_2$ [28], it would result in the formation of liquid phase during heating steps at the high temperatures (above approximately 800 °C). In addition, industrial water glass contains some metallic impurities, such as Fe, the iron-silicon liquid phase probably was formed through the reaction between SiO gas and Fe at the initial stage of reaction. Owing to the existence of these liquid phases at the reaction temperature, SiC seems to have been formed easily by dissolution-precipitation through the liquid phase by the well-known VLS mechanism. Industrial

water glass contains complex composition, so detailed growth mechanism of worm-like SiC is still unclear.

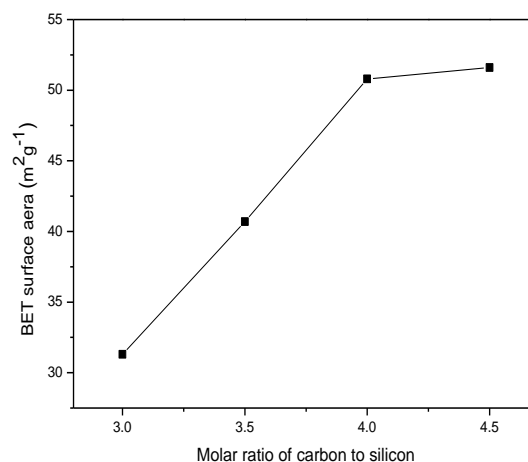


Fig. 4. BET surface area of the worm-like SiC.

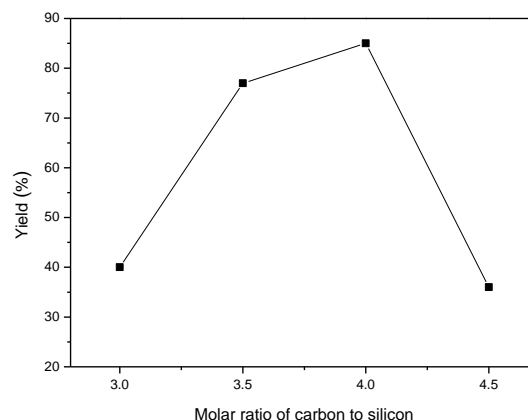


Fig. 5. Yield of the SiC samples.

BET surface areas of the synthesized SiC are shown as Fig. 4. It is obvious that surface area of the products sharply increases with the increase of the molar ratio of carbon to silicon. When molar ratio of carbon to silicon equal to 4, the surface area of synthesized SiC is up to 50.8 m^2/g . Further increase of the carbon content in the precursor does not lead to substantial change in the surface area. This could be due to when the molar ratio of carbon and silicon is 4, carbon and silicon can completely react. Further increase of carbon content can make the amount of liquid phase reduce, thus the solution viscosity increase, the diffusion rate in the reaction reduce and the formed SiC precursor is nonuniform [29].

Fig. 5 shows the yield of the SiC nanofibers. It can be seen that the yield of SiC nanofibers is low when the molar ratio of carbon to silicon is low. When molar ratios of carbon to silicon reach 3.5 and 4, the yields of SiC products are high to 77% and 85%, respectively. High yield of SiC nanofibers is attributed to the complete

reaction of carbon and silicon. Subsequently the yield decrease with the increase of the molar ratio of carbon to silicon.

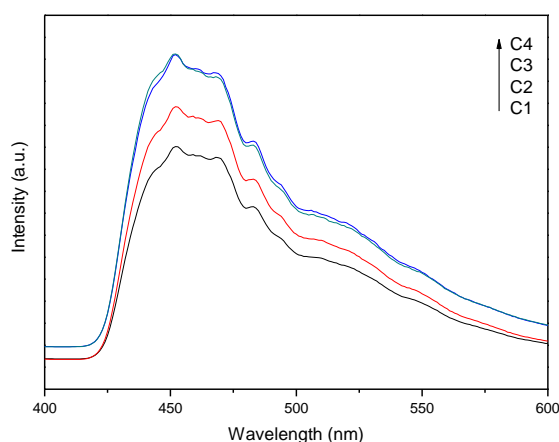


Fig. 6. Room-temperature photoluminescence spectra of the SiC samples.

Fig. 6 displays the PL spectra of the as-obtained SiC under excitation wavelength of 370 nm at room temperature. It is apparent that the overall trend of the PL spectra is similar, and the PL strength firstly increases then decreases with the increase of molar ratio of carbon to silicon. The PL strength of C3 and C4 is very close and both are higher than that of others. The main PL peak is at 450 nm, which is in accordance with the value of the needle-shaped SiC nanowires [15] and SiC nanocrystallites [30] and corresponds to a band gap of 2.76 eV ($1240/\text{wavelength} = \text{eV}$) [4]. This peak is generally regarded as the result of the quantum size effects. In addition, it can be clearly observed that there exists another peak at 468 nm (2.65 eV), which was also found in the needle-shaped 3C-SiC nanowires [31]. Chen [31] believed that the strong peak at 468 nm was ascribed to the effect of morphology, orientation, defects and facets' dangling bonds of the needle-shaped nanowires. Compared with the band gap of bulk 3C-SiC (2.23 eV), the PL spectra here are all considerably blue-shifted. In the spectra, there exists a similar shoulder between 456 nm and 465 nm, which may be the result of microstructures and defects within the nanofibers. Due to its intensive blue-green light emission, SiC nanofibers may have potential application in light emitting diodes, field electron emission and display devices especially for the environment of high temperature and high irradiation.

4. Conclusion

Worm-like SiC nanofibers were successfully synthesized by simple carbothermal reduction of a mixture of phenolic resin and water glass without catalyst. The diameters of worm-like SiC are in the range of 20-110 nm and the maximum lengths are above one micron. The

synthesized worm-like SiC nanofibers have a surface area of 51.6 m²/g. There are stable and intensive PL peaks along 450 nm and 468 nm under excitation wavelength of 370 nm at room temperature, which has considerable blue shifts relative to the bulk 3C-SiC. This could be ascribed to quantum size effects and microstructures and defects within the nanofibers. The SiC preparation technology, using economic raw materials and simple process, will be feasible for future industrial production.

Acknowledgements

This work was supported by a NSFC project (No. 21173251) and a SXICC project (2011SQNRC18).

References

- [1] L. D. Zhang, X. S. Fang, *J. Nanosci. Nanotechnol.* **8**, 149 (2008).
- [2] N. D. Hoa, N. Van Quy, H. Song, Y. Kang, Y. Cho, D. Kim, *J. Cryst. Growth* **311**, 657 (2009).
- [3] K. Yang, Y. Yang, Z. M. Lin, J. T. Li, J. S. Du, *Mater. Res. Bull.* **42**, 1625 (2007).
- [4] J. J. Chen, W. H. Tang, L. P. Xin, Q. Shi, *Appl. Phys. A* **102**, 213 (2011).
- [5] X. T. Li, X. H. Chen, H. H. Song, *Mater. Sci. Eng., B* **176**, 87 (2011).
- [6] M. Bauer, L. Kador, *J. Phys. Chem. B* **107**, 14301 (2003).
- [7] Y. J. Hao, J. B. Wagner, D. S. Su, G. Q. Jin, X. Y. Guo, *Nanotechnology* **17**, 2870 (2006).
- [8] X. N. Guo, R. J. Shang, D. H. Wang, G. Q. Jin, X. Y. Guo, K. N. Tu, *Nanoscale Res. Lett.* **5**, 332 (2010).
- [9] H. X. Zhang, P. X. Feng, V. Makarov, B. R. Weiner, G. Morell, *Mater. Res. Bull.* **44**, 184 (2009).
- [10] B. M. Moshtaghoun, R. Poyato, F. L. Cumbreira, S. de Bernardi-Martin, A. Monshi, M. H. Abbasi, F. Karimzadeh, A. Dominguez-Rodriguez, *J. Eur. Ceram. Soc.* **32**, 1787 (2012).
- [11] H. H. Ye, N. Titchenal, Y. Gogotsi, F. Ko, *Adv. Mater.* **17**, 1531 (2005).
- [12] H. T. Wang, L. Lin, W. Y. Yang, Z. P. Xie, L. N. An, *J. Phys. Chem. C* **114**, 2591 (2010).
- [13] W. M. Zhou, L. J. Yan, Y. Wang, Y. F. Zhang, *Appl. Phys. Lett.* **89**, 013105 (2006).
- [14] X. Y. Guo, G. Q. Jin, Y. J. Hao, *Mater. Res. Soc. Symp. Proc.* **815**, 77 (2004).
- [15] V. G. Pol, S. V. Pol, A. Gedanken, S. H. Lim, Z. Zhong, J. Lin, *J. Phys. Chem. B* **110**, 11237 (2006).
- [16] Y. Zhang, E. W. Shi, Z. Z. Chen, X. B. Li, B. Xiao, *J. Mater. Chem.* **16**, 4141 (2006).
- [17] Q. G. Fu, H. J. Li, X. H. Shi, K. Z. Li, J. Wei, Z. B. Hu, *Mater. Chem. Phys.* **100**, 108 (2006).
- [18] Z. J. Li, H. J. Li, X. L. Chen, A. L. Meng, K. Z. Li, Y. P. Xu, L. Dai, *Appl. Phys. A: Mater. Sci. Process.* **76**, 637 (2003).
- [19] X. H. Sun, C. P. Li, W. K. Wong, N. B. Wong, C. S. Lee, S. T. Lee, B. K. Teo, *J. Am. Chem. Soc.* **124**,

- 14464 (2002).
- [20] T. Seeger, P. Kohler-Redlich, M. Ruhle, *Adv. Mater.* **12**, 279 (2000).
- [21] B. M. Eick, J. P. Youngblood, *J. Mater. Sci.* **44**, 160 (2009).
- [22] L. P. Xin, Q. Shi, J. J. Chen, W. H. Tang, N. Y. Wang, Y. Liu, Y. X. Lin, *Mater. Character.* **65**, 55 (2012).
- [23] D. H. Wang, X. Fu, *J. Optoelectron. Adv. M.* **14**, 478 (2012).
- [24] Y. J. Hao, G. Q. Jin, X. D. Han, X. Y. Guo, *Mater. Lett.* **60**, 1334 (2006).
- [25] D. H. Wang, D. Xu, Q. Wang, Y. J. Hao, G. Q. Jin, X. Y. Guo, K. N. Tu, *Nanotechnology* **19**, 215602 (2008).
- [26] W. S. Seo, K. Koumoto, S. Aria, *J. Am. Ceram. Soc.* **83**, 2584 (2000).
- [27] W. S. Seo, K. Koumoto, S. Aria, *J. Am. Ceram. Soc.* **81**, 1255 (1998).
- [28] M. D. Allendorf, K. E. Spear, *J. Electrochem. Soc.* **148**, B59 (2001).
- [29] J. X. Lin, Y. Zheng, Y. Zheng, K. M. Wei, *Chinese J. Inorg. Chem.* **22**, 1778 (2006).
- [30] J. Y. Fan, X. L. Wu, R. Kong, T. Qiu, G. S. Huang, *Appl. Phys. Lett.* **86**, 171903 (2005).
- [31] J. J. Chen, R. B. Wu, G. Y. Yang, Y. Pan, J. Lin, L. L. Wu, R. Zhai, *J. Alloys Compd.* **456**, 320 (2008).

*Corresponding author: jyty2280@163.com